AD NUMBER

AD851067

NEW LIMITATION CHANGE

TO

Approved for public release, distribution unlimited

FROM

Distribution authorized to U.S. Gov't. agencies and their contractors; Critical Technology; OCT 1968. Other requests shall be referred to Naval Weapons Center, China Lake, CA 93555.

AUTHORITY

USNWC ltr, 24 Mar 1972

NWC TP 4653

THE KALMAN FILTER IN TRANSFER ALIGNMENT OF AIRBORNE INERTIAL GUIDANCE SYSTEMS

by

Arthur A. Sutherland, Jr. and Arthur Gelb
The Analytic Sciences Corporation
for the
Weapons Development Department

ABSTRACT. The problem of transferring alignment between two airborne inertial navigator platforms is treated using the Kalman Filter approach. The important parameters are identified and exercised over a reasonable range to establish accuracy trade-offs. Suggestions are provided for improving the accuracy of Kalman Filter transfer alignment through more complex maneuvers of the carrying aircraft.

NAVAL WEAPONS CENTER
CHINA LAKE, CALIFORNIA • OCTOBER 1968

45

CONTENTS

Section 1. INTRODUCTION

The optimum linear filter developed by Kalman and others is a dynamic means of data processing which is useful in estimating the state of linear systems from noise measurements (Ref. 1). Among the many problems which can be formulated in a manner compatible with the Kalman Filter is the transfer alignment of one inertial guidance platform (slave) to another (master). If it is assumed that alignment to within a few degrees is possible by a means such as gimbal angle matching, the differential equations which describe state variable differences between the two systems are basically linear. The differences which become the state variables of the alignment problem, are random variables as are the inertial sensor errors which cause them to change with time. Certain of these alignment state variables are readily available to use as inputs to the Kalman Filter--that is, they are the measurements. The misalignment angles between the two systems can then be estimated and removed with an accuracy greater than that obtainable through practical mechanical transfer alignment techniques.

This report develops base-line data for use in evaluating proposed equipment and estimation schemes for the transfer alignment problem. The principal quantities of interest are the Kalman Filter errors in estimates of the misalignment angles. It is assumed that correction of the misalignment can be easily carried out with a greater accuracy than the estimation, therefore estimation accuracy is equivalent to alignment accuracy.

Section 2 provides a derivation of the alignment system equations, including all relations necessary to analyze the Kalman Filter accuracy. Section 3 identifies those alignment system parameters which are most important and Section 4 provides trade-off relations between them and alignment time and accuracy. More complex schemes are briefly discussed in Section 5 as the basis for future investigation.

Section 2. DERIVATION OF SYSTEM AND MEASUREMENT EQUATIONS

BASIC ERROR DYNAMICS

The linear equations describing the dynamics of misalignment angles and other important parameters are derived in this chapter for the transfer alignment between two nearly aligned inertial platforms. The systems are assumed to be aligned to within a few degrees before the start of the Kalman Filter operation. Gimbal angle matching techniques are available to perform this coarse alignment and the residual attitude errors are assumed to result from flexure of the structure connecting the two platforms and from mounting errors. The measurements permitted are differences between horizontal velocity indications by the two systems operating independently during filtering. It is assumed that velocity corrections are applied to account for the fact that the two systems may be physically separated by a rotating rigid structure. The slave platform is assumed to be provided with initial values of velocity and position from the master, and the earth rate platform commands applied to the two systems are identical.

It can be seen from Eq. 42, 45, and 50 of Ref. 1 that ideal accelerometers measure the quantity

$$\frac{\bar{f}}{m} = \left[\frac{d^2\bar{R}}{dt^2}\right]_E + 2\,\bar{\Omega} \times \left[\frac{d\bar{R}}{dt}\right]_E - \bar{g} \qquad (1)$$

The vector of master system accelerometer outputs, identified by the subscript M, is

$$\text{master accelerometer outputs} = \left(\frac{\bar{f}}{m}\right)_M + \bar{\nabla}_M \qquad (2)$$

where $\bar{\nabla}_M$ is the vector of master system accelerometer errors. Because the angular misorientation between the slave accelerometer input axes and the corresponding master axes is small it can be represented by a vector of rotation, $\bar{\xi}$. The components of $\bar{\xi}$, ξ_x, ξ_y, and ξ_z, represent the angular rotation about the master axis designated by the subscript which is necessary to bring the master platform into alignment with the slave platform. Since the two systems are closely aligned, the negative of these components describes the rotation about the designated slave

axis necessary to bring the slave system into alignment with the master (the order of rotation is unimportant). Neglecting effects due to separation between the two systems, the vector of slave accelerometer outputs would be

$$\text{slave accelerometer outputs} = \left(\frac{\bar{f}}{m}\right)_M - \bar{\xi} \times \left(\frac{\bar{f}}{m}\right)_M + \bar{\nabla}_S \qquad (3)$$

where $\bar{\nabla}_S$ is the vector of slave accelerometer errors.

It is assumed that the differences between slave and master system velocity indications are corrected for the relative velocity which results from their physical separation on a rotating rigid body. This correction can be computed from knowledge of the aircraft angular velocity and the relative position of the two platforms with respect to the aircraft center of mass. Any errors in this calculation, as well as structural flexure effects, will be viewed as measurement errors in the velocity difference. As a consequence of the velocity correction applied, the difference between Eq. 2 and 3 can be taken as the derivative of the noise-free velocity difference vector, Δv

$$\dot{\overline{\Delta v}} = -\bar{\xi} \times \left(\frac{\bar{f}}{m}\right)_M + \bar{\nabla}_S - \bar{\nabla}_M \qquad (4)$$

If the ideal coordinate axes are aligned north (x), east (y), and down (z) and if the master system is closely aligned to them, we get (Eq. 1)

$$\left(\frac{\bar{f}}{m}\right)_M \cong \begin{bmatrix} a_x \\ a_y \\ a_z \end{bmatrix} + 2 \begin{bmatrix} -\Omega_z v_y \\ \Omega_z v_x - \Omega_x v_z \\ \Omega_x v_y \end{bmatrix} - \begin{bmatrix} 0 \\ 0 \\ g \end{bmatrix} = \begin{bmatrix} a_x - 2\,\Omega_z v_y \\ a_y + 2\left(\Omega_z v_x - \Omega_x v_z\right) \\ \left(a_z - g\right) + 2\,\Omega_x v_y \end{bmatrix} \qquad (5)$$

where a_x, a_y, and a_z are accelerations relative to the earth, v_x, v_y, and v_z are velocities relative to the earth and Ω_x and Ω_z are components of the earth's rotation vector. The magnitude of the terms arising from Coriolis acceleration is very small. For example, if the aircraft has

a velocity of 1,000 ft/sec, the magnitude of $\Omega_x v_y$ cannot exceed 7.3×10^{-2} ft/sec^2. Of course this is much less than the magnitude of g. Similarly, a_x and a_y will be much larger than the corresponding x-axis and y-axis Coriolis terms unless a very straight flight path is maintained. Consequently, though it is not necessary to permit the use of the Kalman Filter in transfer alignment, the Coriolis acceleration terms in Eq. 5 are neglected and Eq. 4 becomes

$$\dot{\overline{\Delta v}} = -\overline{\xi} \times \begin{bmatrix} a_x \\ a_y \\ a_z - g \end{bmatrix} + \overline{\nabla}_S - \overline{\nabla}_M \tag{6}$$

The components of $\dot{\overline{\Delta v}}$ are given by

$$\Delta\dot{v}_x = \left(\nabla_{x_S} - \nabla_{x_M}\right) + a_y \xi_z - \left(a_z - g\right) \xi_y$$

$$\Delta\dot{v}_y = \left(\nabla_{y_S} - \nabla_{y_M}\right) + \left(a_z - g\right) \xi_x - a_x \xi_z$$

$$\Delta\dot{v}_z = \left(\nabla_{z_S} - \nabla_{z_M}\right) + a_x \xi_y - a_y \xi_x \tag{7}$$

The two platforms experience angular rates with respect to inertial space, expressed in their own coordinate frames, by

$$\left(\omega_M\right)_M = \overline{\Omega} + \overline{\rho}_M + \overline{\epsilon}_M$$

$$\left(\omega_S\right)_S = \overline{\Omega} + \overline{\rho}_S + \overline{\epsilon}_S \tag{8}$$

It is assumed that the earth rate rotational commands are the same in both systems. The derivative of the misalignment vector $\overline{\xi}$ is

$$\dot{\overline{\xi}} = \overline{\omega}_S - \overline{\omega}_M \tag{9}$$

The vectors $\bar{\rho}_M$ and $\bar{\rho}_S$ describe the angular rates of master and slave platforms with respect to earth-fixed coordinates and $\bar{\epsilon}_M$ and $\bar{\epsilon}_S$ are the vectors describing respective platform angular rates due to gyro drift.

Equation 9, resolved in the master coordinates, can be expressed as

$$\begin{aligned}\left(\dot{\bar{\xi}}\right)_M &= \left(\bar{\omega}_S\right)_S - \left(\bar{\omega}_M\right)_M + \bar{\xi} \times \left(\bar{\omega}_S\right)_S \\ &\approx \left(\bar{\epsilon}_S - \bar{\epsilon}_M\right) + \left(\bar{\rho}_S - \bar{\rho}_M\right) + \bar{\xi} \times \left(\bar{\omega}_S\right)_S \end{aligned} \tag{10}$$

The angular rates $\bar{\rho}_M$ and $\bar{\rho}_S$ are determined by the velocities indicated in the inertial systems, i.e.,

$$\left(\bar{\rho}_M\right)_M = \begin{bmatrix} \frac{v_{y_M}}{R} \\ \frac{-v_{x_M}}{R} \\ \frac{-v_{y_M} \tan L}{R} \end{bmatrix} \tag{11}$$

$$\left(\bar{\rho}_S\right)_S = \begin{bmatrix} \frac{v_{y_S}}{R} \\ \frac{-v_{x_S}}{R} \\ \frac{-v_{y_S} \tan L}{R} \end{bmatrix} \tag{12}$$

Consequently,

$$\bar{\rho}_S - \bar{\rho}_M = \begin{bmatrix} \frac{\Delta v_y}{R} \\ \frac{-\Delta v_x}{R} \\ \frac{-\Delta v_y \tan L}{R} \end{bmatrix} \tag{13}$$

Approximating $(\bar{\omega}_S)_S$ as an angular rate vector $\bar{\omega}$ (roughly equivalent to $\bar{\Omega} + \bar{\rho}_M$ since in the cross product with the small vector $\bar{\xi}$ only first-order terms will be retained), Eq. 10 and 13 can be combined to give first-order correct expressions for the components of $\dot{\bar{\xi}}$

$$\dot{\xi}_x = \left(\epsilon_{x_S} - \epsilon_{x_M}\right) + \frac{\Delta v_y}{R} + \omega_z \xi_y - \omega_y \xi_z$$

$$\dot{\xi}_y = \left(\epsilon_{y_S} - \epsilon_{y_M}\right) - \frac{\Delta v_x}{R} + \omega_x \xi_z - \omega_z \xi_x$$

$$\dot{\xi}_z = \left(\epsilon_{z_S} - \epsilon_{z_M}\right) - \frac{\Delta v_y \tan L}{R} + \omega_y \xi_x - \omega_x \xi_y \qquad (14)$$

Equations 7 and 14 can be written in vector-matrix form as

$$\begin{bmatrix} \dot{\Delta v}_x \\ \dot{\Delta v}_y \\ \dot{\Delta v}_z \\ \dot{\xi}_x \\ \dot{\xi}_y \\ \dot{\xi}_z \end{bmatrix} = \begin{bmatrix} 0 & 0 & 0 & 0 & -(a_z - g) & a_y \\ 0 & 0 & 0 & (a_z - g) & 0 & -a_x \\ 0 & 0 & 0 & -a_y & a_x & 0 \\ 0 & \frac{1}{R} & 0 & 0 & \omega_z & -\omega_y \\ -\frac{1}{R} & 0 & 0 & -\omega_z & 0 & \omega_x \\ 0 & \frac{-\tan L}{R} & 0 & \omega_y & -\omega_x & 0 \end{bmatrix} \begin{bmatrix} \Delta v_x \\ \Delta v_y \\ \Delta v_z \\ \xi_x \\ \xi_y \\ \xi_z \end{bmatrix} + \begin{bmatrix} v_{x_S} - v_{x_M} \\ v_{y_S} - v_{y_M} \\ v_{z_S} - v_{z_M} \\ \epsilon_{x_S} - \epsilon_{x_M} \\ \epsilon_{y_S} - \epsilon_{y_M} \\ \epsilon_{z_S} - \epsilon_{z_M} \end{bmatrix} \qquad (15)$$

A block diagram illustration of Eq. 15 is shown in Fig. 1.

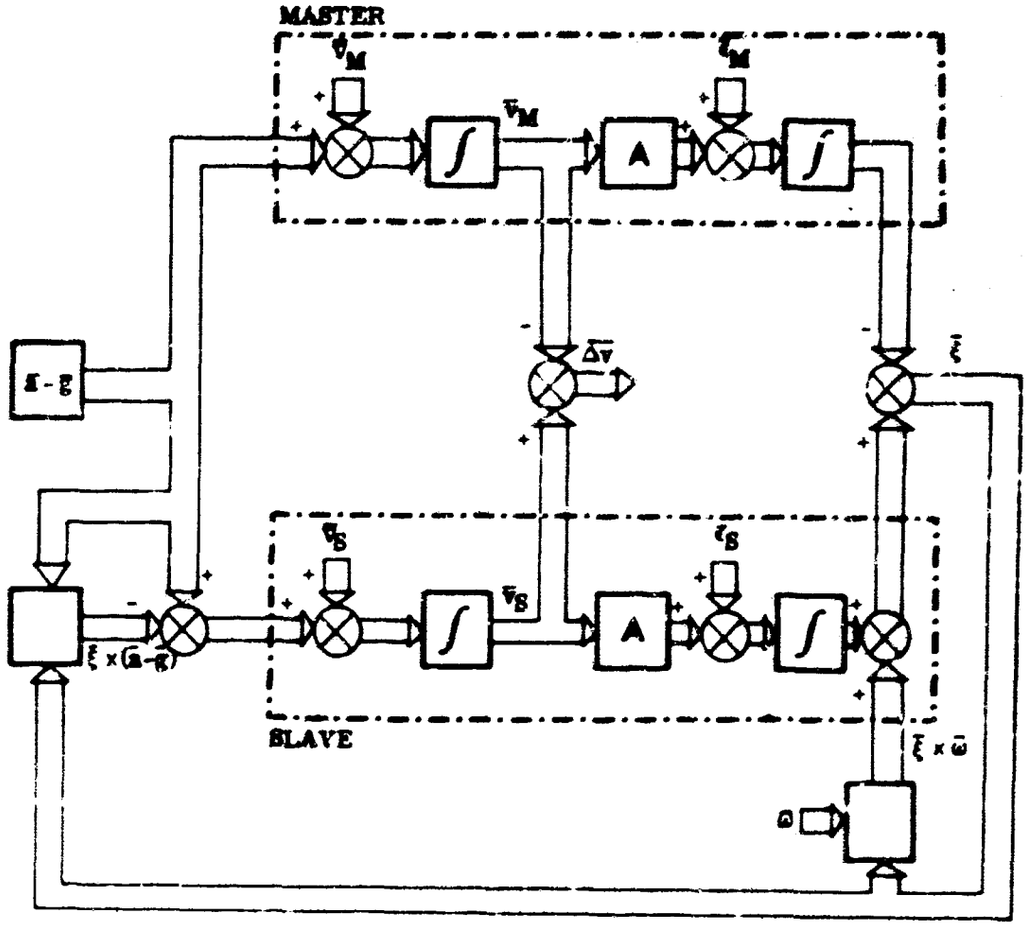

$$\mathbf{A} = \begin{bmatrix} 0 & \frac{1}{R} & 0 \\ -\frac{1}{R} & 0 & 0 \\ 0 & \frac{-\tan L}{R} & 0 \end{bmatrix}$$

FIG. 1. Illustration of Equation 15.

The measurements provided to the Kalman Filter are the velocity differences Δv_x, Δv_y, and Δv_z. The measurement matrix for the state vector in Eq. 15 is

$$H = \begin{bmatrix} 1 & 0 & 0 & 0 & 0 & 0 \\ 0 & 1 & 0 & 0 & 0 & 0 \\ 0 & 0 & 1 & 0 & 0 & 0 \end{bmatrix} \tag{16}$$

The velocity comparison scheme is illustrated in Fig. 2.

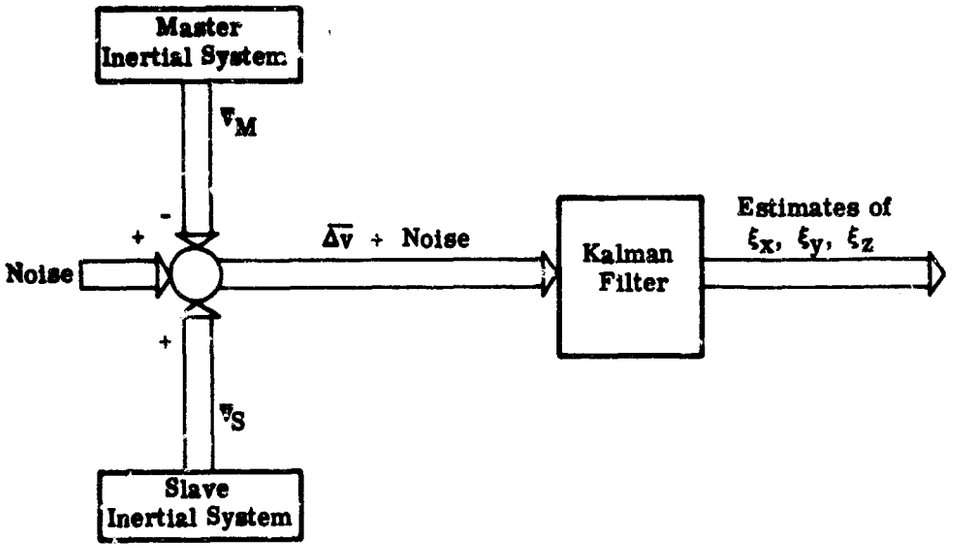

FIG. 2. Velocity Comparison for Kalman Filter Transfer Alignment.

Frequently the vertical axis of near-earth inertial navigators is instrumented by means other than inertial sensors. This is a consequence of the basic instability which exists in computing vertical position and velocity from accelerometer measurements (see Appendix C of Ref. 1). When other means of z-axis instrumentation are provided, $\Delta \dot{v}_z$ becomes independent of the other quantities in the state vector of Eq. 15. The third row in the matrix contains only zeros. The third column in the matrix is also zero and Eq. 15 can be written in the uncoupled form

$$\begin{bmatrix} \dot{\Delta v}_x \\ \dot{\Delta v}_y \\ \dot{\xi}_x \\ \dot{\xi}_y \\ \dot{\xi}_z \end{bmatrix} = \begin{bmatrix} 0 & 0 & 0 & -(a_z - g) & a_y \\ 0 & 0 & (a_z - g) & 0 & -a_x \\ 0 & \frac{1}{R} & 0 & \omega_z & -\omega_y \\ -\frac{1}{R} & 0 & -\omega_z & 0 & \omega_x \\ 0 & \frac{-\tan L}{R} & \omega_y & -\omega_z & 0 \end{bmatrix} \begin{bmatrix} \Delta v_x \\ \Delta v_y \\ \xi_x \\ \xi_y \\ \xi_z \end{bmatrix} + \begin{bmatrix} \nabla_{x_S} - \nabla_{x_M} \\ \nabla_{y_S} - \nabla_{y_M} \\ \epsilon_{x_S} - \epsilon_{x_M} \\ \epsilon_{y_S} - \epsilon_{y_M} \\ \epsilon_{z_S} - \epsilon_{z_M} \end{bmatrix} \tag{17}$$

$$\Delta \dot{v}_z = \left(\nabla_{z_S} - \nabla_{z_M} \right) \tag{18}$$

Equation 18 is of no value in determining the misalignment angles ξ_x, ξ_y, and ξ_z. Equation 17 is the basis for the linear description of error (state) dynamics used in most of the transfer alignment studies in this report. The corresponding measurement matrix is given by

$$H = \begin{bmatrix} 1 & 0 & 0 & 0 & 0 \\ 0 & 1 & 0 & 0 & 0 \end{bmatrix} \tag{19}$$

The gyro and accelerometer errors shown in Eq. 17 are highly correlated in time. Because the Kalman Filter formulation presented in Section 2 of Ref. 1 permits only uncorrelated system disturbances, the state vector must be augmented to include the inertial sensor errors. It is assumed that the time to perform a practical transfer alignment is on the order of a minute or two and the gyro and accelerometer errors will remain essentially constant over that period. The augmented state vector dynamics are described by

$$\begin{bmatrix} \dot{\Delta v}_x \\ \dot{\Delta v}_y \\ \dot{\xi}_x \\ \dot{\xi}_y \\ \dot{\xi}_z \\ \dot{\nabla}_x \\ \dot{\nabla}_y \\ \dot{\epsilon}_x \\ \dot{\epsilon}_y \\ \dot{\epsilon}_z \end{bmatrix} = \left[\begin{array}{ccccc|c} 0 & 0 & 0 & -(a_z - g) & a_y & \\ 0 & 0 & (a_z - g) & 0 & -a_x & \\ 0 & \frac{1}{R} & 0 & \omega_z & -\omega_y & I_5 \\ -\frac{1}{R} & 0 & -\omega_z & 0 & \omega_x & \\ 0 & \frac{-\tan L}{R} & \omega_y & -\omega_x & 0 & \\ \hline & & & & & \\ & & O_5 & & & O_5 \\ & & & & & \end{array}\right] \begin{bmatrix} \Delta v_x \\ \Delta v_y \\ \xi_x \\ \xi_y \\ \xi_z \\ \nabla_x \\ \nabla_y \\ \epsilon_x \\ \epsilon_y \\ \epsilon_z \end{bmatrix} \tag{20}$$

where I_5 and O_5 are the 5 × 5 identity and zero matrices, respectively, and

$$\nabla_x = \nabla_{x_S} - \nabla_{x_M}$$

etc. Notice that the state vector differential equation (Eq. 20) has no forcing terms. The corresponding measurement matrix is

$$H = \begin{bmatrix} 1 & 0 & 0 & 0 & 0 & 0 & 0 & 0 & 0 & 0 \\ 0 & 1 & 0 & 0 & 0 & 0 & 0 & 0 & 0 & 0 \end{bmatrix} \tag{21}$$

KALMAN FILTER ACCURACIES

The use of the Kalman Filter to estimate the state variables of a linear system from linear measurements permits easy calculation of the covariance matrix of the estimation errors. Because system velocity differences are provided continuously, the matrix Riccati differential equation for the error covariance matrix (Eq. 29 of Ref. 1) is used

$$\dot{P} = FP + PF^T - PH^TR^{-1}HP + GQG^T \tag{22}$$

The lack of random forcing terms in Eq. 20 permits simplification of Eq. 22

$$\dot{P} = FP + PF^T - PH^TR^{-1}HP \tag{23}$$

The matrices F and H are given in Eq 20 and 21. The matrix R and initial conditions on the error covariance remain to be specified.

Measurement Errors

The matrix R is the covariance of the measurement error vector $\underline{v}$ described in the measurement equation

$$\underline{z} = H\underline{x} + \underline{v} \tag{24}$$

For the state vector and measurements described under Basic Error Dynamics (p. 2), the measurement error vector $\underline{v}$ is composed of errors in indications of the differences between indicated north and east velocities of the slave and master inertial platforms. Velocity differences due to physical separation of the two platforms are removed by compensating the measurement under the assumption that the connecting structure is rigid. Flexure of this structure will provide uncompensated random velocity differences, generally of a high-frequency nature relative to the system response. These errors, in addition to data processing and signal transmission noise can be viewed as measurement errors. A third potential velocity difference error arises from the use of Doppler velocity measurements in the master inertial system. All three effects are of such a high-frequency nature relative to system dynamics that they will be considered uncorrelated. Together they provide the measurement error $\underline{v}$. Because the elements of $\underline{v}$ are north and east velocity difference errors while the structural vibration and Doppler velocity errors are usually expressed in

vehicle axes, the off-diagonal elements of R are generally non-zero and dependent on vehicle orientation relative to the navigation coordinates. However, for simplicity the two elements of the measurement error vector will be assumed to have no cross-correlation in the study which follows. Under the assumptions outlined above, the combined effects of vibration, data noise, and Doppler errors will be described by a single quantity, the diagonal element of the R matrix, r,

$$R = \begin{bmatrix} r & 0 \\ 0 & r \end{bmatrix} \tag{25}$$

It will be sufficient for the purposes of this study to vary the magnitude of r without specifying its separate contributing sources. (Indeed, measurement error sources may arise in addition to those discussed above.) For example, if the contributions of each system to the elements of $\underline{v}$, v_1, and v_2 are assumed to have flat spectral density with bandwidth of 1,000 cps and RMS magnitude of 1.5 ft/sec, Eq. 177 and 178 of Ref. 1 indicate that

$$r \cong \frac{2(1.5 \text{ ft/sec})^2}{\left(2\pi \times 10^3 \frac{1}{\text{sec}}\right)} + \frac{2(1.5 \text{ ft/sec})^2}{\left(2\pi \times 10^3 \frac{1}{\text{sec}}\right)} = 1.43 \times 10^{-3} \ (\text{ft}^2/\text{sec}^2) \text{ sec}$$

Initialization

Specification of the initial estimation error covariance matrix is simplified by the assumption that there is no cross-correlation between estimation errors at the start of filtering. This is a reasonable assumption although the flexure modes of the carrying vehicle may produce some correlation between the initial values of misalignment angles ξ_x, ξ_y, and ξ_z. The diagonal elements of $P(t_o)$ are the mean square errors in the initial estimates of the state variables. In the case of the velocity differences Δv_x and Δv_y, it is assumed that the master velocities are provided for initializing the slave system and that the RMS errors in this initialization are equal to the RMS errors introduced in the velocity difference between the two systems. For example, using the velocity indication errors described above,

$$P_{11}(t_o) = P_{22}(t_o) = (1.5 \text{ ft/sec})^2 + (1.5 \text{ ft/sec})^2 = 4.50 \text{ ft}^2/\text{sec}^2$$

The mean square errors in the initial estimates of ξ_x, ξ_y, and ξ_z are taken as the mean square misalignment errors between the two systems. The three variances are chosen to be equal under the assumption that the factors contributing to initial misalignment are the same along each of the navigation system axes. For example, if the RMS misalignment errors were two degrees about each axis,

$$P_{33}(t_o) = P_{44}(t_o) = P_{55}(t_o) = 1.22 \times 10^{-3} \text{ rad}^2$$

The diagonal elements of $P(t_o)$ corresponding to the last five state variables in Eq. 20 can be easily computed from the mean square inertial sensor errors. Assuming all gyro drift rates and accelerometer errors to be random constants with zero means and to be independent from one instrument to another,

$$P_{66}(t_o) = \nabla^2_{x_S} + \nabla^2_{x_M} \tag{26}$$

where $\nabla^2_{x_S}$ and $\nabla^2_{x_M}$ are the mean square slave x accelerometer and master x accelerometer errors, respectively. The remaining diagonal elements are calculated in an analogous manner.

Equation 26 illustrates an important aspect of transfer alignment. To the extent that inertial sensor errors limit transfer alignment accuracy or practicality, if one inertial platform contains sensors whose RMS errors are much larger than the other system's, no improvement of the more accurate set of inertial sensors will improve transfer alignment significantly. Accuracy in this case is limited by the quality of the poorest set of sensors.

As an example of the calculation of the lower five diagonal elements in the initial error convariance matrix, consider an RMS slave accelerometer bias of 5×10^{-5} g (1.61×10^{-3} ft/sec^2) and an RMS bias in the corresponding master sensor of 10^{-5} g (3.22×10^{-4} ft/sec^2). The diagonal element is computed according to Eq. 26

$$\left\{\begin{matrix} P_{66} \\ \text{or} \\ P_{77} \end{matrix}\right\} = \left(1.61 \times 10^{-3}\right)^2 + \left(3.22 \times 10^{-4}\right)^2 \cong \left(1.61 \times 10^{-3}\right)^2$$

$$= 2.59 \times 10^{-6} \frac{\text{ft}^2}{\text{sec}^4}$$

It can be seen that the slave sensor error dominates these terms.

The section concludes with the observation that many of the elements in the system matrix, F, as displayed in Eq. 20 may be time-varying and dependent on the velocity and acceleration of the vehicle carrying both inertial systems. It will be shown later that these elements of the F matrix play an important role in determining transfer alignment accuracy and practicality.

Section 3. IDENTIFICATION OF IMPORTANT PARAMETERS

A large number of parameters exert potential influence on the Kalman Filter accuracy in the transfer alignment problem. If a study is to proceed efficiently it must systematically determine which parameters are important over the range of values considered and which may be held constant at a reasonable value. Once the important parameters have been identified, they will be exercised within specified limits and trade-off relations will be determined.

VELOCITY AND POSITION MATCHING

The first simplification to be discussed involves transfer alignment implementation rather than inertial system parameters. In addition to the velocity-matching scheme discussed in Section 2, it is also possible to compare position indications from the two inertial systems and use the differences obtained to estimate misalignment. In terms of the matrices presented in Section 2, this scheme adds two additional rows and columns on the top and left side of F. The new elements are all zeros except for ones in the third column of the first new row and the fourth column of the second new row. The H matrix also contains two additional rows and columns. They are added on the right and lower sides and consist of ones in the third column of the third row and fourth column of the fourth row, and zeros elsewhere. The R matrix is expanded to dimension 4 × 4 and the new state variables Δp_x and Δp_y are placed at the top of the state vector. Of course, the error covariance matrix also contains an additional two rows and two columns.

The implementation of the Kalman Filter in the case where position-matching is used involves a larger F matrix. However, the significant increase in complexity results from doubling the number of inputs to the filter (measurements). The addition of two new state variables and the new measurements raises the filter gain matrix size from 20 elements (2 × 10) for velocity-matching to 48 elements (4 × 12) when position- and velocity-matching are used.

To evaluate the relative accuracy between the two schemes, the error covariance equation (Eq. 23) was used to determine RMS alignment accuracies. In one case both position and velocity comparison were used, while in the other only the velocities were compared. The initial misalignments, accelerometer bias errors, and velocity measurement errors used are those presented in Section 2.[1] The RMS slave gyro drift

[1] Appendix B contains a table of important variables for each computer solution of Eq. 23 discussed in this document.

rates were taken to be 0.05 deg/hr and the master gyro drift rates were assumed much smaller. When position-matching was used, the RMS initial error in position difference and the RMS position difference measurement error were identical to the values for the corresponding velocity differences. (Of course the units are different.) With the additional assumption that the position difference errors have the same frequency distribution as described earlier for velocity errors, the elements of R and P(0) corresponding to position differences are also the same as those for velocity differences. The aircraft carrying the two systems was assumed to be in level flight heading due east with a velocity of 1,000 ft/sec. (Aircraft heading has no influence on alignment accuracy. See Ref. 2.)

Figures 3 and 4 show the RMS estimation error histories of the north level and azimuth misalignment angles, respectively. The calculations represented a total estimation time of 5 minutes but the north level error reached its lower boundary in less than 1 minute.[2] East level misalignment behaved in the same manner. The combination of position- and velocity-matching provides more rapid convergence of the estimates on the true values but does not result in greater accuracy than velocity-matching alone.

While the accuracy in the estimate of azimuth misalignment improves by more than an order of magnitude, the RMS value of ξ_z is still much larger than those for the two level misalignment angles. A scheme must be sought to reduce the RMS error in the azimuth misalignment angle to the same magnitude as the level errors. This must also be accomplished within a reasonable time period if it is to be useful for an airborne missile. In the next section it will be demonstrated that greater accuracy in the estimate of ξ_z, together with a filter time on the order of 1 minute, can be achieved using velocity-matching alone. Consequently, the remainder of this report will concentrate on this much simpler scheme. The combination of sufficient accuracy, rapid convergence, and relative simplicity make the velocity-matching approach considerably more attractive than the comparison of both position and velocity.

HORIZONTAL MANEUVERS

If the aircraft which carries the two inertial guidance platforms is permitted to perform maneuvers in the horizontal plane only, the optimum maneuver is a high acceleration turn (Ref. 2). This maneuver minimizes the sum of the mean square estimation errors of the three misalignment angles. The major benefit of the turning maneuver is its ability to aid the Kalman Filter in accurate estimation of azimuth

[2] The lower limit of the RMS north level estimation error, 5×10^{-5} rad, results from the RSS east accelerometer bias error of 5×10^{-5} g according to the discussion in Section 9 of Ref. 1.

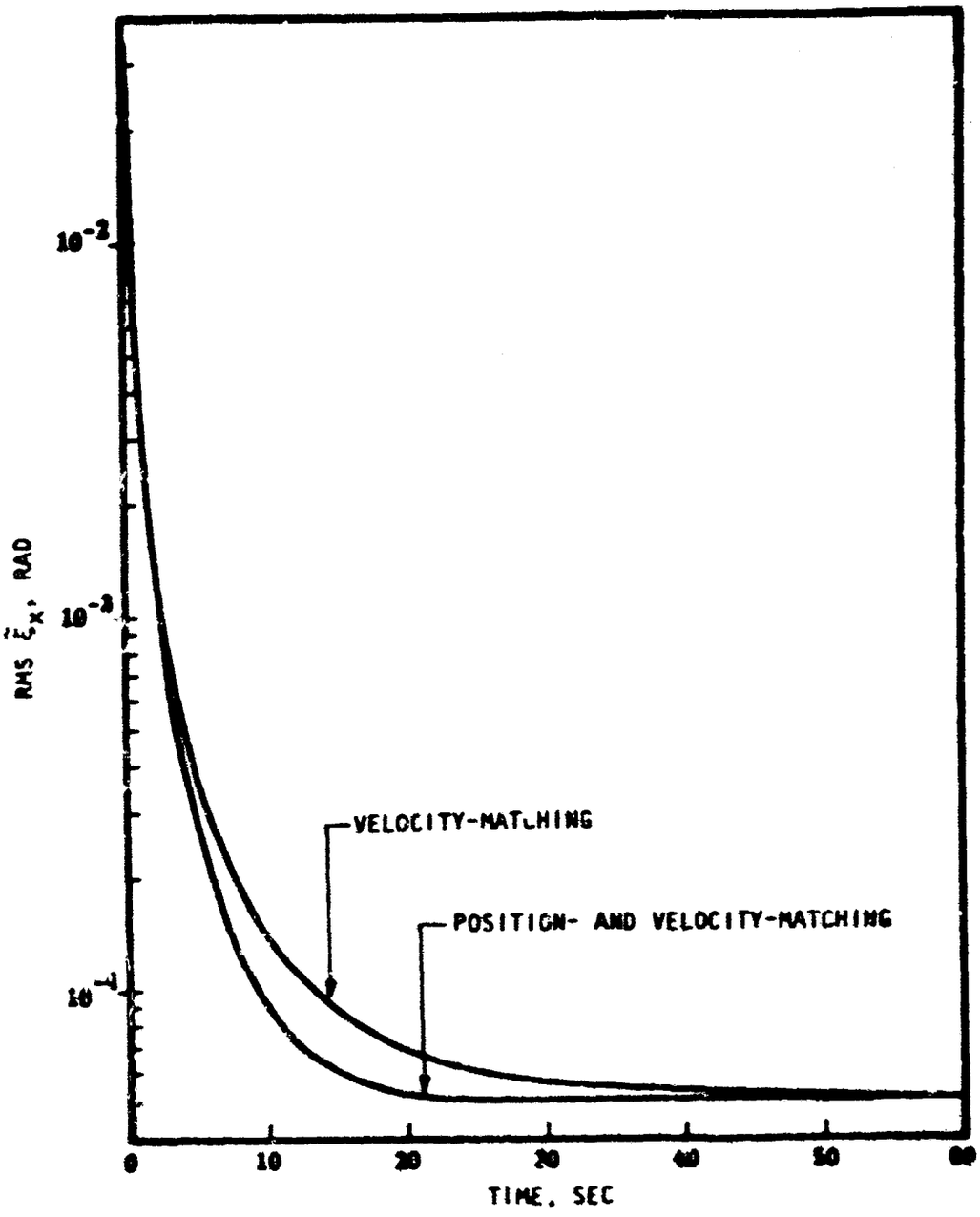

FIG. 3. Comparison of Position and Velocity Matching With Velocity Matching Kalman Filter Accuracies.

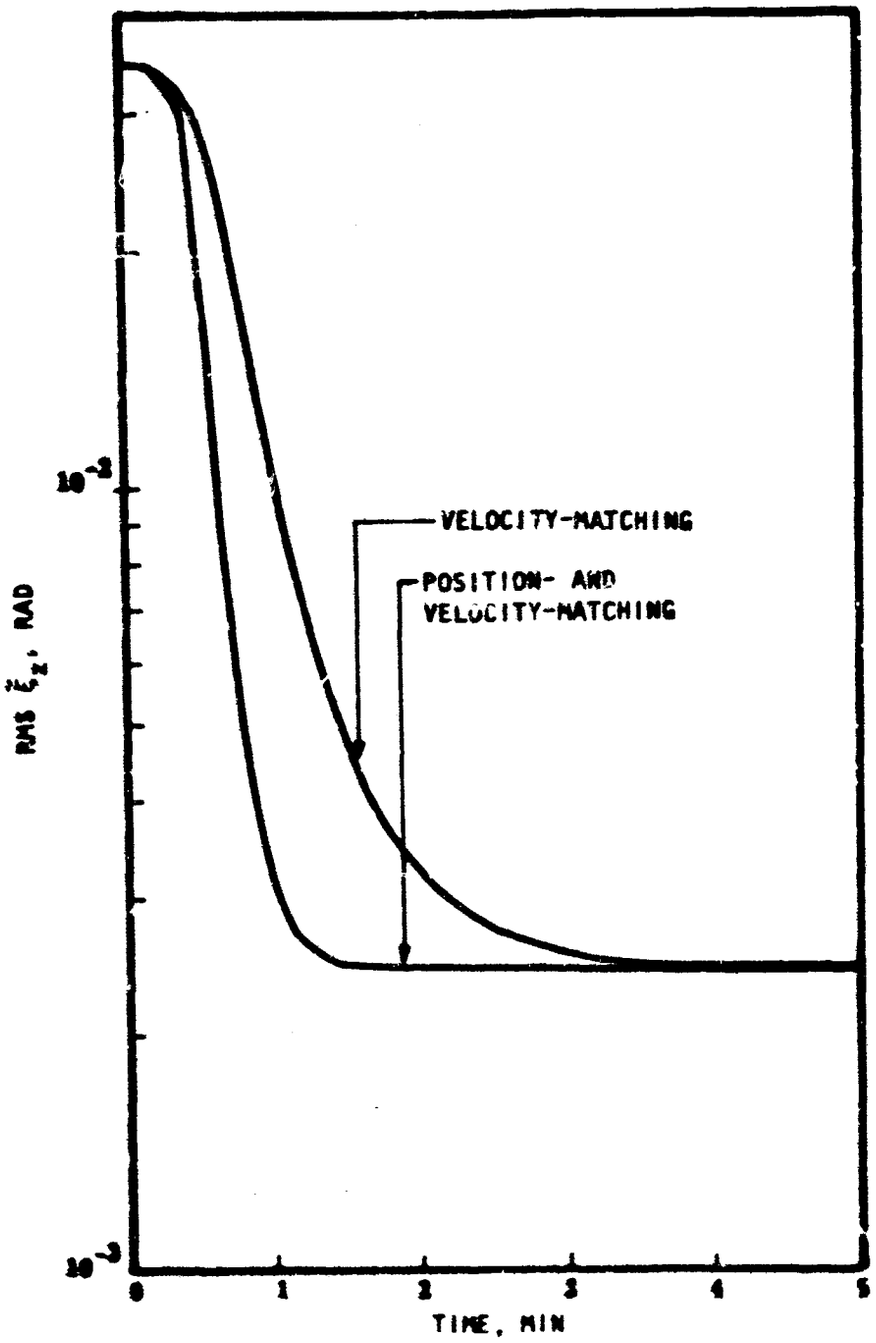

FIG. 4. Comparison of Position and Velocity Matching With Velocity Matching Kalman Filter Accuracies.

misalignment. This is illustrated in Fig. 5. As the horizontal acceleration due to a turning maneuver increases from 0 to 3 g, the filter accuracy increases dramatically. The time histories shown were computed using Eq. 23 with the initial conditions and measurement error magnitude already presented. In all cases the turn began when the aircraft was heading due south. Reference 2 indicates that initial heading is not significant. Only velocity matching was considered. Because the 3-g horizontal acceleration (3.2-g total acceleration) is considered a reasonable maximum and because the best total misalignment accuracy is obtained with that maneuver, all results reported hereafter will be for such a maneuver unless otherwise stated. In addition, all parameters will be the same as those presented above unless different values are given.

GYRO DRIFT RATE

The effect of gyro drift rate was investigated by repeating the calculations for the 3-g turn with the larger RMS slave gyro drift rate of 0.5 deg/hr. This order-of-magnitude larger gyro drift rate produced an increase in the sum of the RMS misalignment estimation errors at the end of 50 seconds to 1.65 times their original value. Most severely affected was the RMS azimuth misalignment error which rose from 1.04×10^{-5} rad to 3.12×10^{-5} rad. However, since the latter value is still less than the lower limit on the level angle estimation errors, this increase is less significant than it might otherwise seem. The level angle estimation errors did not increase as dramatically because they had essentially reached their lower limit in less than 50 seconds when the original gyro drift rate value of 0.05 deg/hr was used. Within the range described, gyro drift rate does not appear to exert a very significant influence on the Kalman Filter accuracy. Consequently, all subsequent results will be obtained assuming the lower value for slave gyro drift rate.

INITIAL MISALIGNMENT ERRORS

The effect of the initial misalignment errors on the Kalman Filter accuracy and filtering time was studied by increasing the RMS initial misalignment errors (as reflected in the appropriate diagonal elements of P(0)) from 2 to 4 deg/axis. Again, Eq. 23 was used to determine time histories of error statistics. No significant increase was found in the misalignment estimation errors at the end of 10 seconds. It is concluded that the RMS value of initial misalignment errors has no effect on Kalman Filter accuracy in the parameter range of interest. The RMS magnitude of 2 deg/axis will be used in all subsequent calculations.

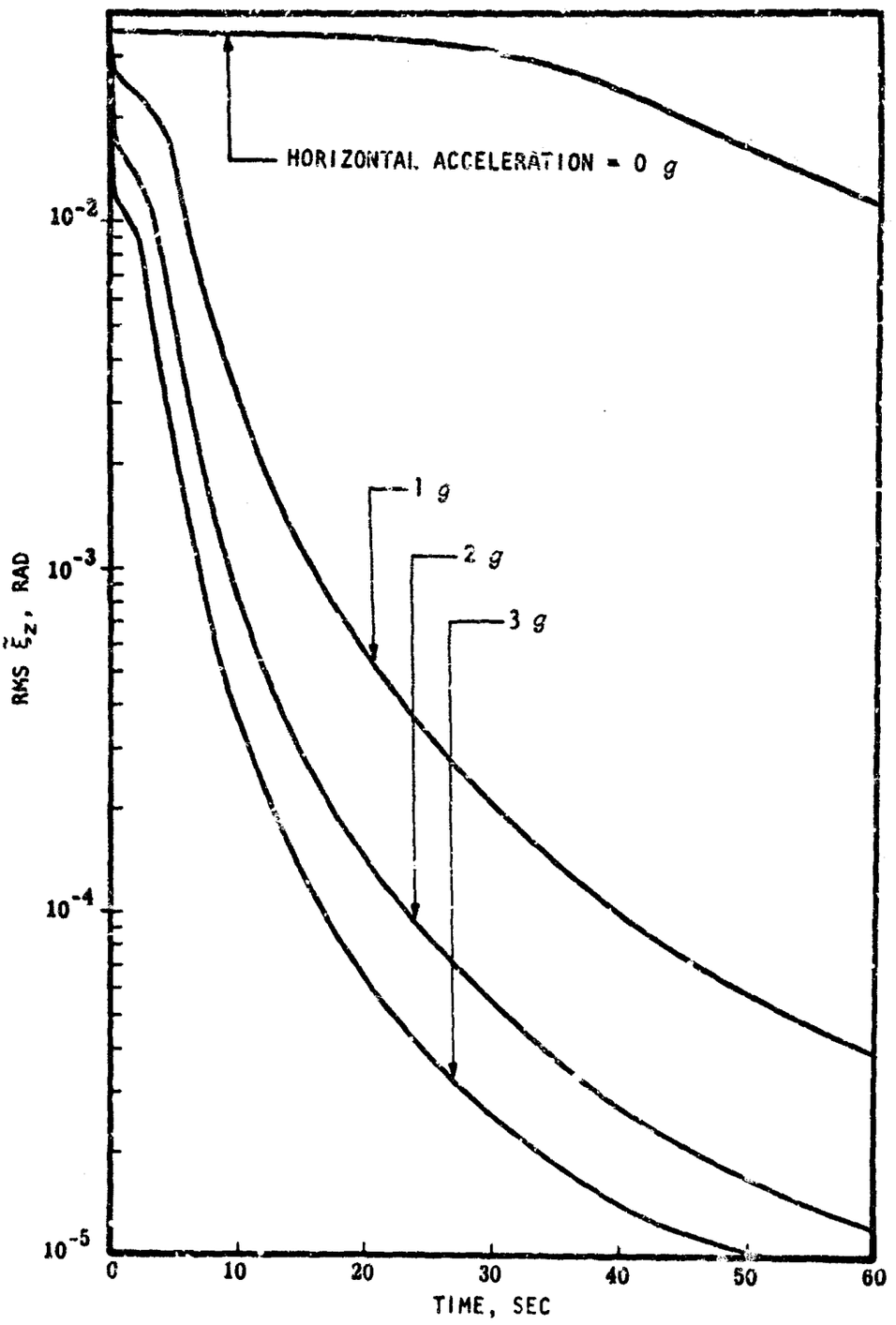

FIG. 5. Velocity Matching: Effect of Horizontal Acceleration on Kalman Filter Accuracy.

ACCELEROMETER BIAS ERROR

As already discussed, the RMS slave accelerometer bias error provides a lower limit for the accuracy of Kalman Filter estimates of level errors if the aircraft is restricted to move in the horizontal plane. Consequently, it is not surprising that raising the RMS bias value by an order of magnitude increases the RMS level angle estimation errors at the end of 50 seconds by a factor of 10. Of course, the simple relation which results is also a consequence of the fact that in both cases the errors in level angle estimates have reached the lower limit at the end of 50 seconds of filtering. Figure 6 shows the north level error time histories for the two bias values.[3] No significant change in azimuth angle estimation accuracy resulted from changing the level accelerometer bias errors. Obviously, at least for the case where the aircraft is restricted to horizontal motion during alignment, slave accelerometer bias errors are important.

MEASUREMENT NOISE

It is of particular interest to observe the effect of variations in measurement noise as expressed in the diagonal elements of the R matrix. Not only is the measurement noise amplitude to be encountered in a practical application not well known, but the elements of R represent a combination of mean square measurement errors and the spectral distribution of these errors. Consequently, variation of this parameter (diagonal element, r) is necessary to provide a basis for predicting filter accuracy when these characteristics are subsequently determined. Figures 7 and 8 illustrate the effect of measurement errors on the ability of the Kalman Filter to rapidly provide accurate estimates of the misalignment angles. The larger value of the R matrix diagonal element, r, represents measurement errors with an RMS amplitude 8 times that represented by the smaller value, both having the same spectral distribution. The larger measurement error causes a slower convergence of the Kalman Filter estimates on the true values of the misalignment angles. A more complete presentation of the effects of measurement errors is deferred until the next section.

[3] Throughout the report figures illustrating effects on level angle estimation accuracy will be drawn for ξ_x, the angle about the north axis. However, all conclusions apply also to ξ_y which exhibits almost identical behavior.

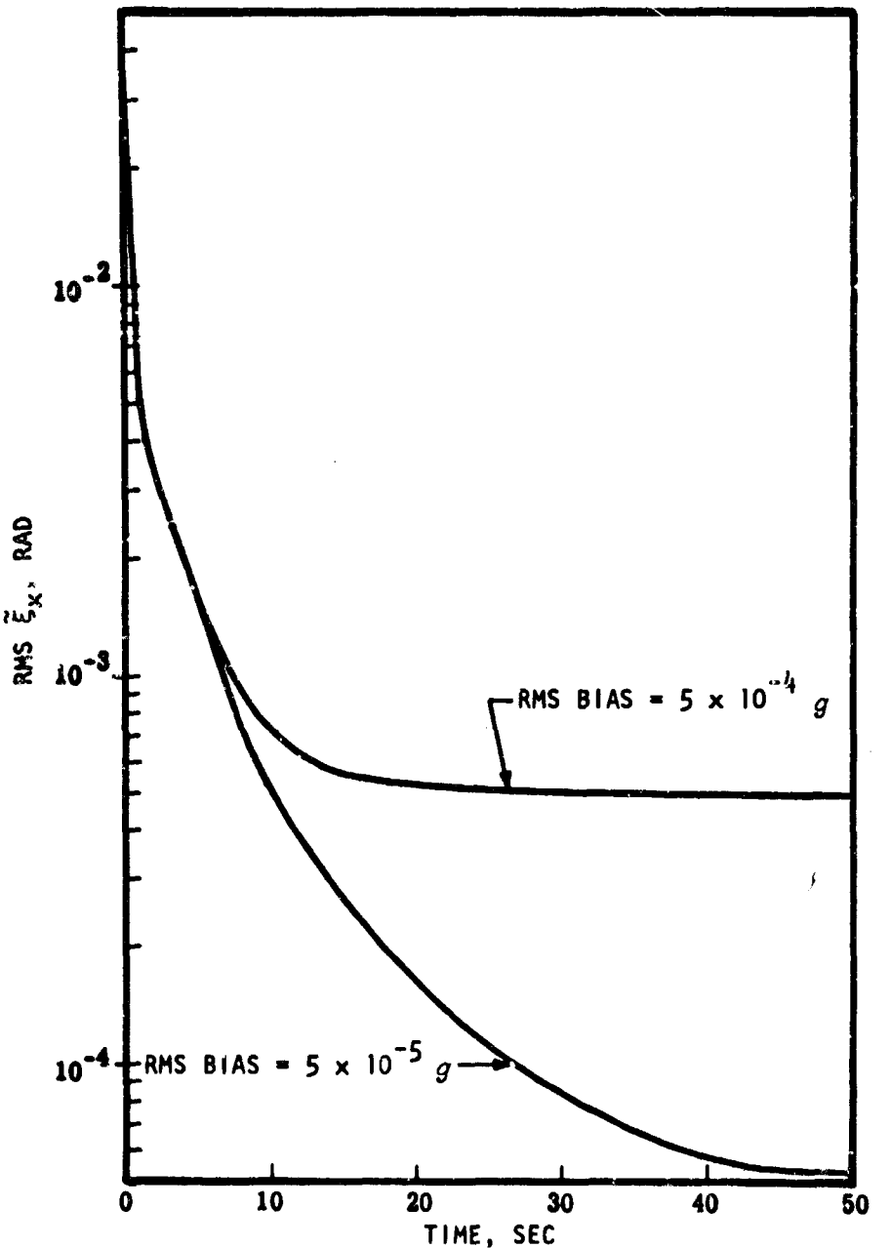

FIG. 6. Velocity Matching: Effect of Accelerometer Bias on Kalman Filter Accuracy.

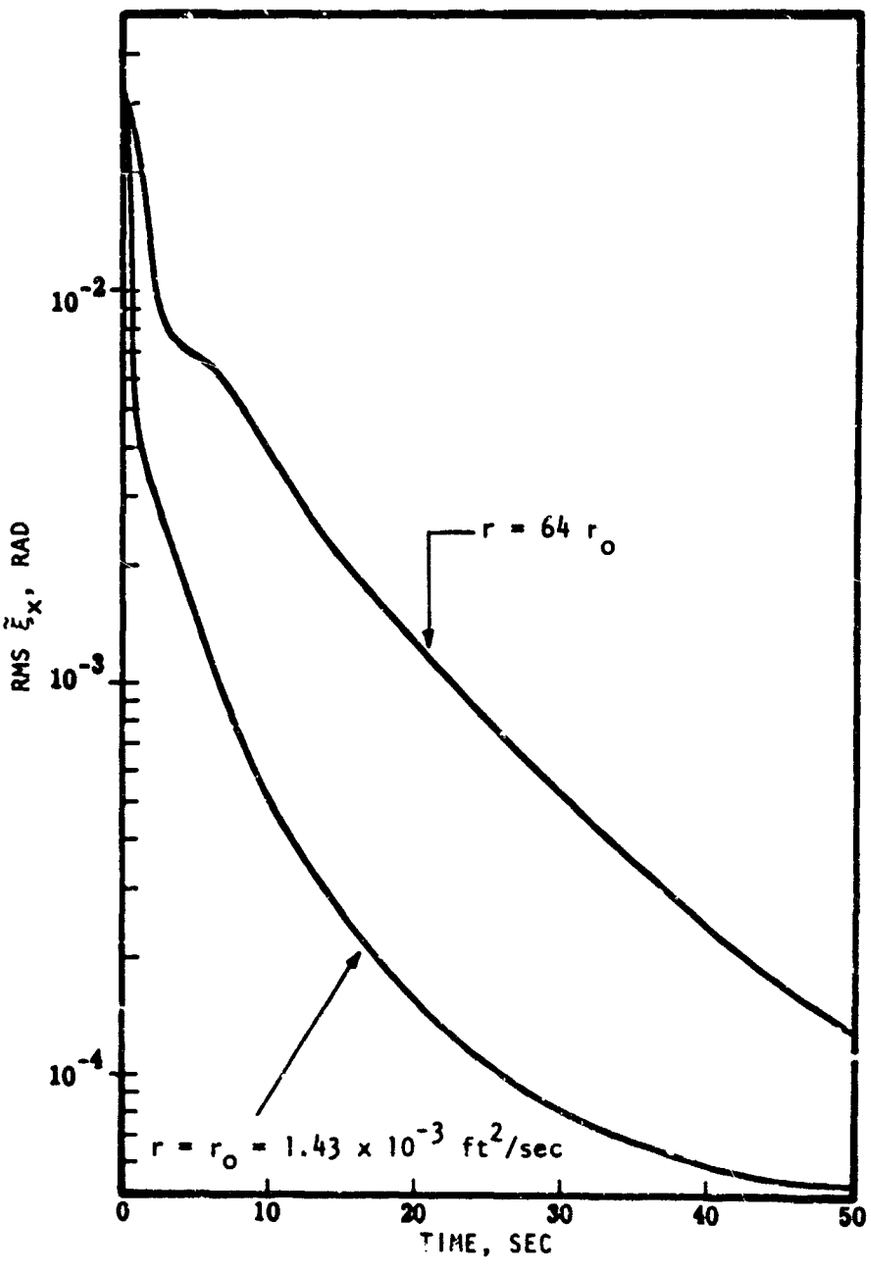

FIG. 7. Velocity Matching: Effect of Measurement Noise on Kalman Filter Accuracy.

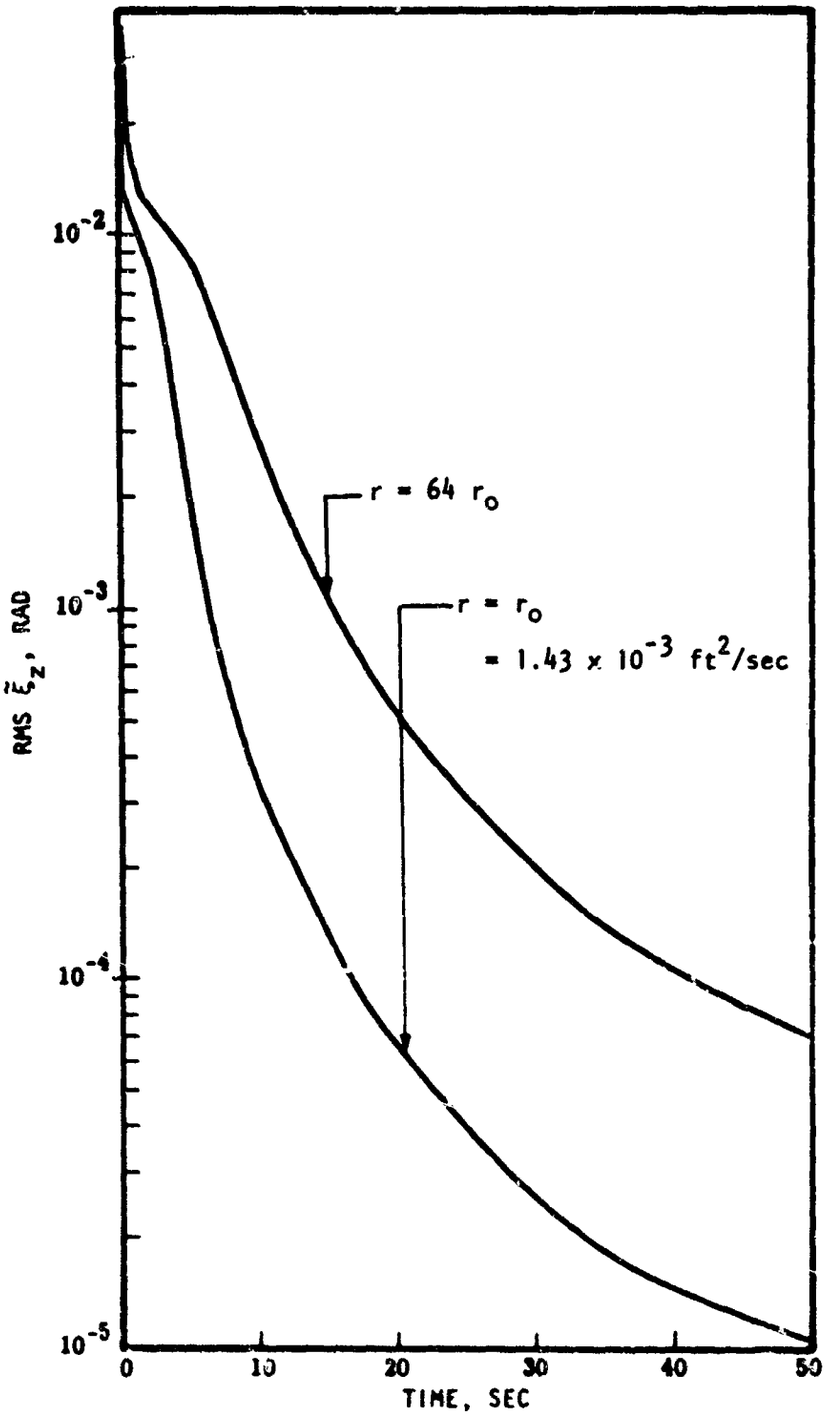

FIG. 8. Velocity Matching: Effect of Measurement Errors.

VEHICLE VELOCITY

The aircraft forward velocity maintained during the horizontal turning maneuver was lowered to 500 ft/sec--half the value assumed in all other computer runs. The major effect of changing vehicle velocity, assuming the same horizontal acceleration is maintained, is to double the frequency of the sinusoidal horizontal acceleration and angular rate components in the F matrix. The estimation accuracies computed using Eq. 23 showed only a slight improvement over those obtained when the velocity was 1,000 ft/sec. It is concluded that, over this range of values, the forward speed of the aircraft carrying the two inertial platforms have little effect on the Kalman Filter alignment accuracy.

INSTRUMENT ERROR CALIBRATION

When the Kalman Filter is used to estimate inertial navigation system errors, the possibility exists for simultaneously estimating the inertial sensor errors--instrument error calibration. Unfortunately, during all the short-time (less than 90 seconds) alignment runs made in the course of this investigation, no significant improvement in the accuracy of sensor error estimates was obtained. The only exception during the entire study occurred when position and velocity differences were used for a period of 5 minutes. In that case the x-axis and y-axis gyro drift rates were reduced by a considerable factor. The possibility of inertial sensor calibration during Kalman Filter alignment of the type discussed appears remote. Gyro drift rates cause errors in position and velocity to grow too slowly for detection in a reasonable filtering time and the initial level errors are so large relative to the accelerometer errors considered that no improved estimate can be made when a horizontal maneuver is prescribed. Section 5 discusses the possibility of using other techniques to help calibrate sensor errors.

It is concluded that the principal parameters which determine Kalman Filter alignment accuracy when the aircraft is flying in a horizontal turn are accelerometer bias errors and velocity difference measurement errors. Consequently, the following section will concentrate on establishing accuracy trade-offs involving these two quantities.

Section 4. TRADE-OFFS INVOLVING IMPORTANT PARAMETERS

ACCELEROMETER BIAS ERRORS

The accelerometer bias errors were varied over a range of values between 5×10^{-5} and 5×10^{-4} g. All other parameters were identical with those used in establishing the filter accuracies displayed in Fig. 5. The aircraft carrying the two inertial platforms was assumed to be performing a horizontal turning maneuver with a horizontal acceleration of 3 g. Figure 9 illustrates the RMS north level estimation error for different filtering times over the range of accelerometer bias errors. The lower limit of these errors as a function of bias is the straight line indicated on the figure. The lines representing 30, 40, and 50 seconds of filtering reach this limit as the bias error nears the upper bound of the range investigated. The principal effect of accelerometer bias on Kalman Filter accuracy is, of course, this lower bound on the level estimation accuracy when the aircraft is restricted to maneuver in the horizontal plane (and only north and east velocities are compared). (See Section 5.) The fact that the curves representing filter accuracy for different filtering times slope upward indicates that larger accelerometer bias errors increase the filtering time required to reach a prescribed accuracy. As mentioned in the previous section, accelerometer bias errors have no appreciable effect on azimuth angle estimation accuracy.

MEASUREMENT ERRORS

Measurement error amplitude and bandwidth, as reflected in the R matrix diagonal elements, affects the speed with which the Kalman Filter estimates converge on the true values of the misalignment angles. A discussion of this effect is found on page 20 of Ref. 1. Figures 10 and 11 illustrate the accuracy trade-offs between velocity difference measurements and the Kalman Filter estimate of level misalignment. The measurement error standard deviation, σ_v, was varied between 1/2 and 8 times the value used in most calculations thus far. Again, the lower limit imposed on estimation accuracy by accelerometer bias errors is evident. For a bias error of 5×10^{-5} g the Kalman Filter accuracy at the end of 10 seconds is linearly related to the RMS measurement noise, σ_v. In all cases the differential change in the RMS estimation error for a given filtering time, de, is related to a differential change in σ_v by

$$de = \left(d\,\sigma_v\right)^b$$

where the exponent b is ≤ 1. As the accelerometer bias error or the filtering time are allowed to increase within the range investigated,

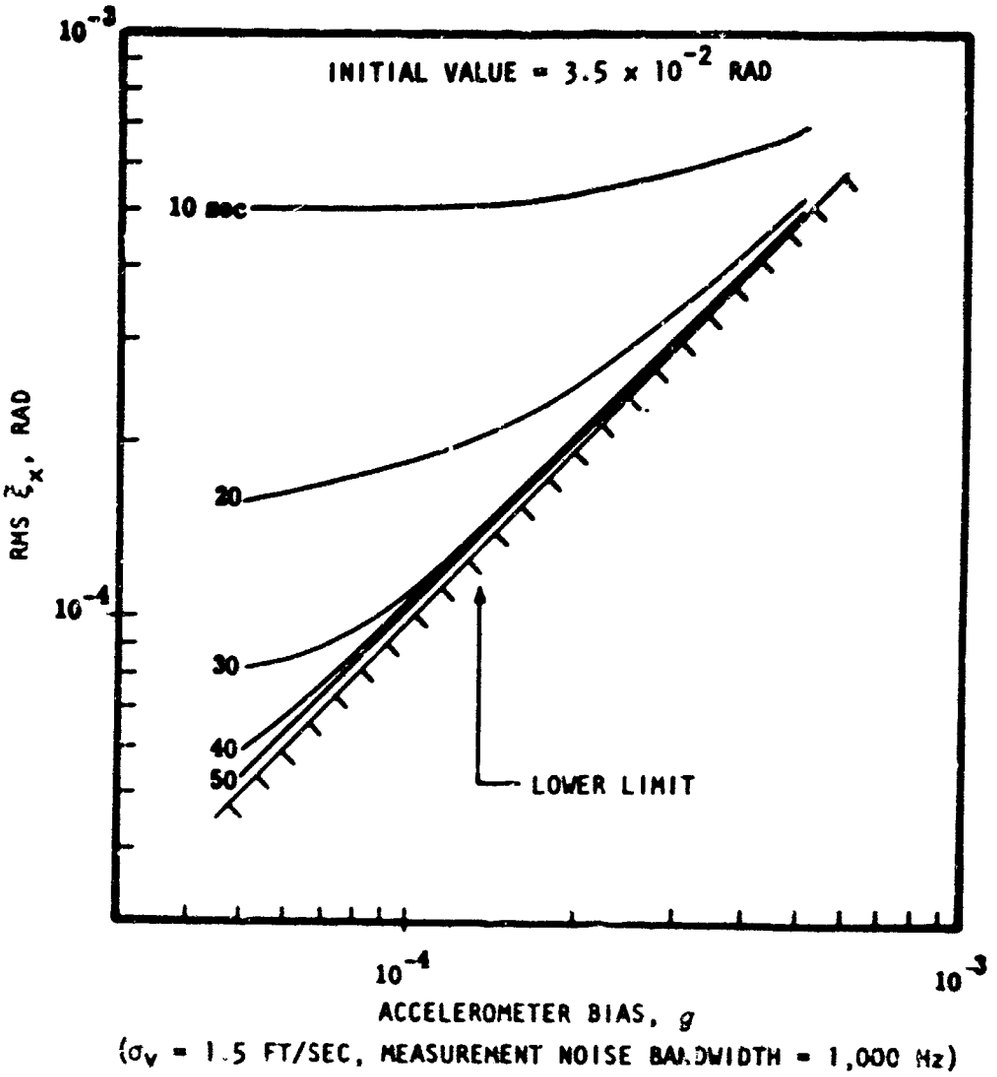

FIG. 9. Velocity Matching: Effect of Accelerometer Bias on Kalman Filter Accuracy.

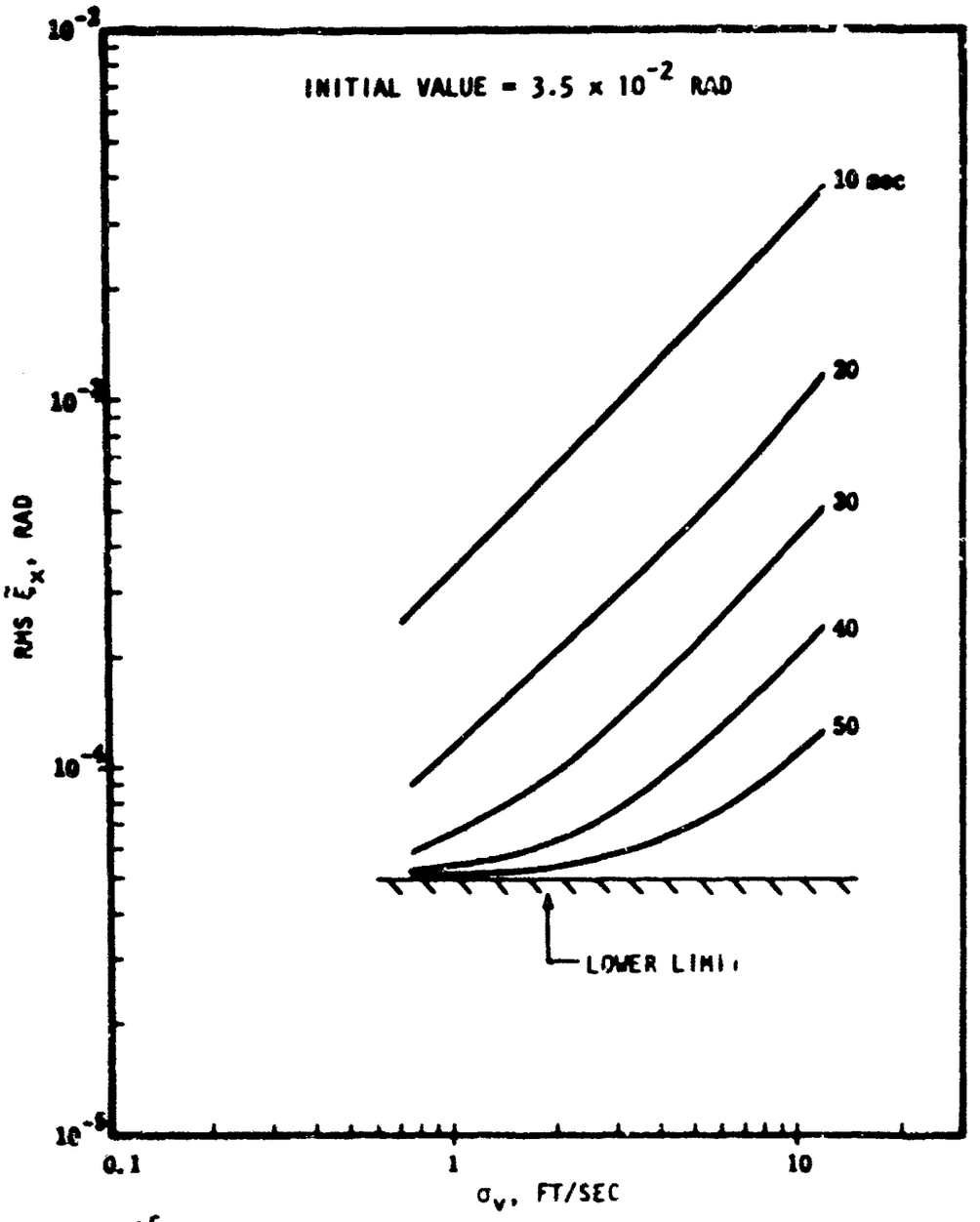

($\nabla_S = 5 \times 10^{-5}$ *g* PER ACCELEROMETER, MEASUREMENT NOISE BANDWIDTH = 1,000 Hz)

FIG. 10. Velocity Matching: Effect of Measur ent Noise on Kalman Filter Accuracy.

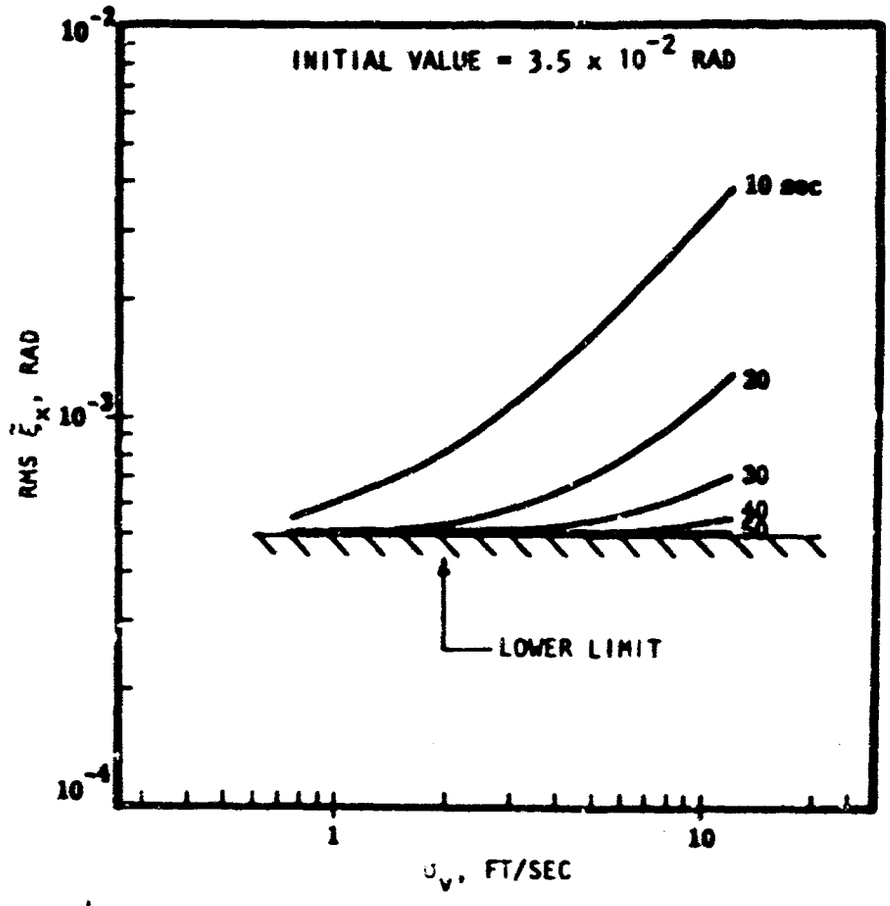

(σ_S = 5 x 10^{-4} g PER ACCELEROMETER, MEASUREMENT NOISE BANDWIDTH = 1,000 Hz)

FIG. 11. Velocity Matching: Effect of Measurement Noise on Kalman Filter Accuracy.

the size of b decreases. This is also a consequence of the limiting effect on level estimation accuracy provided by bias errors: if filtering time and accelerometer error are such that the limit is reached before the end of filtering, a considerable increase in measurement errors must take place before the level errors become larger than the limit.

Figure 12 illustrates the effect of varying the diagonal elements of the R matrix on azimuth error estimation accuracy. The relations are essentially independent of accelerometer bias. The curves of equal estimation time indicate that the relation between azimuth angle estimation accuracy and RMS measurement errors is linear for fixed filtering duration and measurement error bandwidth. Since the parameter varied to obtain these relations was r, not σ_v, the accuracy also varies inversely as the square root of bandwidth when σ_v is fixed. Only the 40-second and 50-second curves show a departure from the first-order relation. They curve at the low values of σ_v, indicating a somewhat less than linear effect in that region of parameters. In the area encompassing small measurement errors and long filtering times the accuracy of the azimuth misalignment estimate approaches a non-zero steady-state value which is not dependent on measurement noise alone. In particular, the gyro drift rates are also important in establishing the steady-state RMS error in ξ_z. However, over almost the entire range of σ_v and filtering time explored, the accuracy of the azimuth error estimate and the velocity difference measurement are linearly related through a constant determined by the measurement error bandwidth and the duration of the filtering process.

Figures 9 through 12 provide useful trade-offs for preliminary determination of the Kalman Filter alignment accuracies possible with proposed systems.

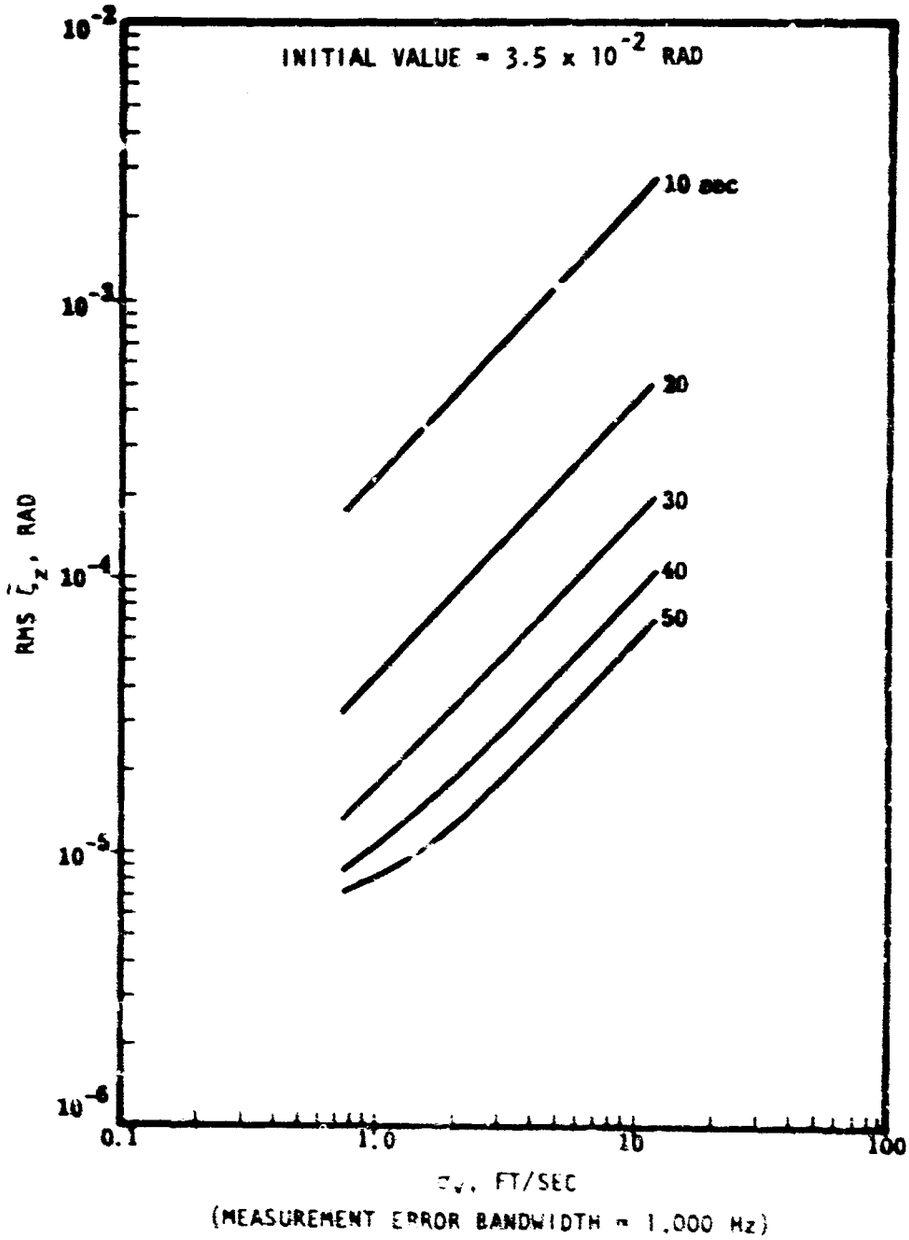

FIG. 12. Velocity Matching: Effect of Measurement Noise on Kalman Filter Accuracy.

Section 5. CONSIDERATION OF VERTICAL MANEUVERS

Depending on the accuracy desired, the Kalman Filter transfer alignment of a slave inertial platform with parameters within the ranges explored in this report may not be satisfactory. In particular, the lower limit on level error estimation accuracy imposed by accelerometer bias errors may be restrictive. Also, depending on the mission time anticipated, the inability to calibrate gyros and accelerometers can be prohibitive. Techniques exist for simultaneously removing most of these objections. They have been investigated in Ref. 2 and found to be very useful.

VERTICAL MANEUVERS

The use of a vertical maneuver during alignment permits the separate observation of accelerometer bias and level error in the horizontal velocity differences. Vertical accelerations generated provide a time-varying characteristic for the $(a_z - g)$ element in the system matrix of Eq. 17 where formerly only the constant quantity, g, appeared. The level error angles then generate time-varying contributions to the measurements Δv_x and Δv_y. These can be distinguished from the constant contributions of accelerometer bias errors without increasing the size of the Kalman Filter. The result, as described in Ref. 2, is the removal of the lower limit on level error estimation accuracy and the ability to calibrate the accelerometers. The improvements obtained depend to a great measure on the relative values of inertial sensor errors and measurement errors. If the gyro drift rates and velocity difference measurement errors permit potential filter accuracies much better than those imposed by the accelerometer bias during a horizontal maneuver, considerable improvement results from providing vertical as well as horizontal motion during filtering.

Figure 13 shows the reduction in the sum of the mean square errors in $\hat{\xi}_x$, $\hat{\xi}_y$, and $\hat{\xi}_z$ that was achieved by following a horizontal turn with a sinusoidal or "porpoise" maneuver in the vertical plane. The abscissa is the peak vertical acceleration achieved, $a_{z_{max}}$. At the start of the vertical maneuver the sum of mean square errors was approximately 4×10^{-6} rad^2. Most of the reduction was achieved in the estimation errors for level angles ξ_x and ξ_y. The addition of vertical maneuvers can provide dramatic improvements in alignment accuracy.

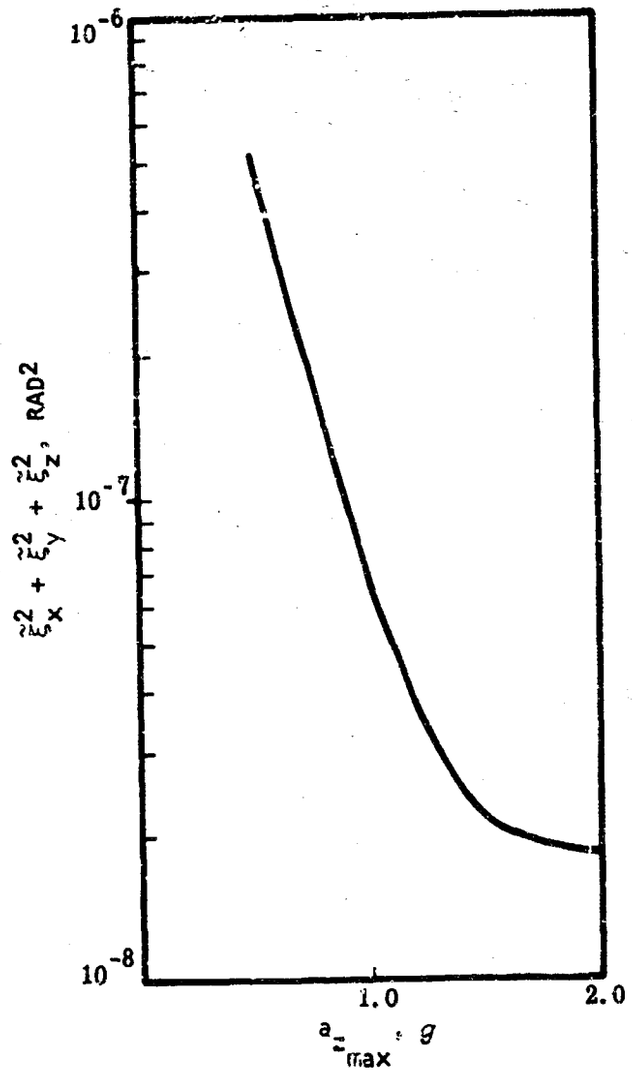

FIG. 13. Sum of Mean Square Misalignment Estimate Errors Versus $a_{z_{max}}$ for 15-Second Porpoise Maneuver (Source: Ref. 2).

z-AXIS VELOCITY COMPARISON

If vertical accelerometers are available, another approach exists for removing the restriction on level angle estimation accuracy. Without employing an additional vertical maneuver, the z-axis velocity difference can be used by the Kalman Filter. The basic formulation is based on Eq. 15. Time-varying indications of level misalignment appear separately in the vertical velocity difference. Consequently, they can be separated from the contributions of accelerometer bias errors. The filter gain matrix of the complete Kalman Filter contains 36 elements instead of the 20 needed for the approach used in Sections 3 and 4. Increased complexity is traded for the ability to achieve more accurate misalignment estimates during a horizontal turn.

Reference 2 indicates that the results of z-axis velocity comparison are essentially the same as for the vertical maneuver--better calibration of accelerometers and removal of the relation between bias errors and level estimate errors discussed in Section 3.

Section 6. CONCLUSIONS

The use of the Kalman Filter to permit estimation of misalignment between two inertial guidance platforms has been explored. Equations were derived describing the linear dynamics of the errors involved and all the necessary matrices were developed.

It was determined that horizontal maneuvering of the carrying aircraft is necessary to provide accurate estimates of azimuth error and alignment times on the order of a minute. The most important parameters within the range investigated were accelerometer bias errors and velocity difference measurement errors. For the principal scheme explored, the accelerometer bias imposes a lower limit on the filter's ability to estimate level misalignment angles. The velocity difference errors help to determine the speed with which the filter estimate converges on the true values. In particular, a linear relation was found to exist between errors in the azimuth angle estimate and measurement accuracies. No improvement in inertial sensor calibration resulted when the basic scheme was applied. Trade-off curves were established relating the misalignment estimate accuracies to accelerometer bias errors, measurement errors, and filter times.

Finally, alternative techniques were discussed briefly and reference was made to other work which demonstrated their usefulness. These approaches involved vertical as well as horizontal aircraft maneuvers and the comparison of z-axis velocities during horizontal turns. It is concluded that these other schemes are useful but somewhat more complex to implement.

Appendix A

ALIGNMENT ERRORS IN THE MASTER SYSTEM AT THE TIME OF TRANSFER ALIGNMENT

In the common circumstance where the slave inertial guidance system is of poorer quality than the master system, all the errors in the latter are incorporated into the former at the conclusion of transfer alignment. Unless the steering commands to the weapon containing the slave system are always provided in the coordinate frame defined by the master system (and therefore include errors provided to the slave during alignment), the nature of master system errors at the time of transfer alignment is important. For this reason one set of such errors was computed for the situation in which the aircraft had been cruising for 1 hour prior to initiation of the alignment procedure. It is emphasized that this set of master system errors is highly dependent on the inertial sensor errors postulated, and especially on the kinds and method of combination of external navigation information used to improve the master inertial system accuracy during flight. The only aid assumed in this example is Doppler velocity information. This external measurement is employed in an optimal manner through the use of a Kalman Filter. Though in actual practice the Doppler information may be time-averaged before use (Ref. 3), for the calculations presented here it is considered as a continuous measurement with high-frequency noise.

The carrying aircraft is assumed to have cruised due east in level flight with a velocity of 1,000 ft/sec for 1 hour prior to alignment. The following parameter descriptions were used:

Latitude, deg	45
Doppler measurement noise (unbiased), ft/sec RMS (across- and along-track with a bandwidth of 1 Hz)	3
Initial master misalignment angles, mrad RMS	2
Initial master position error, ft RMS	10
Initial master velocity error, ft/sec RMS	2
Master accelerometer error, g RMS (exponentially-correlated with a 10-hr correlation time)	10^{-6}
Master gyro drift rate, deg/hr RMS (exponentially-correlated with a 10-hr correlation time)	10^{-2}

The error covariance matrix differential equation was solved by numerical integration and at the end of 1 hour of flight the RMS errors in the master inertial navigator were calculated to be:

Position, ft	
North	411
East	919
Velocity, ft/sec	
North	0.13
East	0.05
Level, rad	
North	5.0×10^{-6}
East	1.1×10^{-5}
Azimuth, rad	1.1×10^{-4}

The large position errors occur because no external position fixes were made during the flight. If initialization of the slave system with respect to position in earth-fixed coordinates is important, some consideration must be made for providing external position measurements to the master navigator prior to transfer alignment. Of course, addition of position measurements would only serve to further reduce the other master system errors as well. No significant inertial sensor error calibration occurred during this cruise flight.

The fact that RMS errors in all other quantities decreased during the course of the 1-hour flight illustrates the self-alignment capability of the Doppler velocity aided master inertial navigator. It can be seen that, for the range of values investigated in Section 4, the transfer alignment attitude errors are of the same order of magnitude as those already present in the master inertial system at the start of alignment.

Appendix B

TABLE OF PARAMETERS

Table 1 shows the values of all important parameters specified in the computer solutions of Eq. 23 which are discussed in this report. The section, and in most cases the figure, in which the results for each parameter group are summarized are listed in the first column.

TABLE 1. Parameter Groups

Reference	Horizontal acceleration, g	RMS $(\varepsilon_S - \varepsilon_M)$ per gyro, deg/hr	RMS $(V_S - V_M)$, per accelerometer, g	RMS initial misalignment angle, per axis, deg	RMS measurement noise, per axis, per system (1,000 Hz bandwidth), ft/sec
Velocity and Position Matching (p. 15); Fig. 2 and 3	0	5×10^{-2}	5×10^{-5}	2.0	1.5 ft/sec (velocity match) 1.5 ft (position match)
Horizontal Maneuvers (p. 16); Fig. 4	0 to 3	5×10^{-2}	5×10^{-5}	2.0	1.5
Gyro Drift Rate (p. 19)	3	5×10^{-1}	5×10^{-5}	2.0	1.5
Initial Misalignment Errors (p. 19)	3	5×10^{-2}	5×10^{-5}	4.0	1.5
Accelerometer Bias Error (p. 21); Fig. 5	3	5×10^{-2}	5×10^{-4}	2.0	1.5
Measurement Noise (p. 21) Fig. 6 and 7	3	5×10^{-2}	5×10^{-5}	2.0	12.0
Accelerometer Bias Error (p. 26); Fig. 8	3	5×10^{-2}	5×10^{-5} to 5×10^{-4}	2.0	1.5
Measurement Errors (p. 26); Fig. 9 and 11	3	5×10^{-2}	5×10^{-5}	2.0	0.75 to 12.0
Measurement Errors (p. 26); Fig. 10	3	5×10^{-2}	5×10^{-4}	2.0	0.75 to 12.0

NOTE: In all cases the RMS initial error in velocity difference (and position difference, if used) is 1.5 ft/sec (or ft) per axis, per system. In all cases except that reported under Vehicle Velocity (p. 25) the aircraft speed was 1,000 ft/sec.

REFERENCES

1. Naval Weapons Center. Application of the Kalman Filter to Aided Inertial Systems, by Arthur A. Sutherland, Jr. and Arthur Gelb, The Analytic Sciences Corporation. China Lake, Calif., NWC, October 1968. (NWC TP 4652).

2. Sutherland, Arthur A., Jr. Application of Optimal Linear Estimation to the Alignment of Inertial Guidance Systems, Sc.D. Thesis, MIT. Department of Aeronautics and Astronautics, September 1966.

3. International Business Machines Corporation. Synergistic Naviation System Study, by Kenneth A. Klementis, et al. Owego, N.Y., IBM, October 1966. (Report No. 67-928-7).

UNCLASSIFIED

Security Classification

DOCUMENT CONTROL DATA - R & D

Security classification of title, body of abstract and indexing annotation must be entered when the overall report is classified

1 ORIGINATING ACTIVITY (Corporate author) The Analytic Sciences Corporation 6 Jacob Way Reading, Mass.	2a. REPORT SECURITY CLASSIFICATION UNCLASSIFIED 2b GROUP ---

3 REPORT TITLE

THE KALMAN FILTER IN TRANSFER ALIGNMENT OF AIRBORNE INERTIAL GUIDANCE SYSTEMS.

4 DESCRIPTIVE NOTES (Type of report and inclusive dates)
Final Report

5 AUTHOR(S) (First name, middle initial, last name)
Arthur A. Sutherland, Jr.
Arthur Gelb

6 REPORT DATE October 1968	7a TOTAL NO OF PAGES 40	7b NO OF REFS 3
8a CONTRACT OR GRANT NO N60530-67-C-1052 b PROJECT NO AirTask A36533205/216-1/F009-03-03 c d	9a ORIGINATOR'S REPORT NUMBER(S) NWC TP 4653 9b OTHER REPORT NO(S) (Any other numbers that may be assigned this report)	

10 DISTRIBUTION STATEMENT

THIS DOCUMENT IS SUBJECT TO SPECIAL EXPORT CONTROLS AND EACH TRANSMITTAL TO FOREIGN GOVERNMENTS OR FOREIGN NATIONALS MAY BE MADE ONLY WITH PRIOR APPROVAL OF THE NAVAL WEAPONS CENTER.

11 SUPPLEMENTARY NOTES	12 SPONSORING MILITARY ACTIVITY Naval Weapons Center China Lake, Calif. 93555

13 ABSTRACT

The problem of transferring alignment between two airborne inertial navigator platforms is treated using the Kalman Filter approach. The important parameters are identified and exercised over a reasonable range to establish accuracy trade-offs. Suggestions are provided for improving the accuracy of Kalman Filter transfer alignment through more complex maneuvers of the carrying aircraft.

DD FORM 1473

UNCLASSIFIED

Security Classification

14 KEY WORDS	LINK A		LINK B		LINK C	
	ROLE	WT	ROLE	WT	ROLE	WT
Inertial navigator alignment Kalman Filter						